# COMPARISON OF MOVING BOUNDARY AND FINITE-VOLUME HEAT EXCHANGER MODELS IN THE MODELICA LANGUAGE

Adriano Desideri[1*], Bertrand Dechesne[1], Jorrit Wronski[2], Martijn van den Broek[3], Gusev Sergei[3]
Sylvain Quoilin[1], Vincent Lemort[1]

[1] University of Liège, Thermodynamics laboratory,
Campus du Sart Tilman, Liège, Belgium
adesideri@ulg.ac.be

[2] Technical University of Denmark, Department of Mechanical Engineering,
Kongens Lyngby, Denmark

[3] University of Gent, Department of Flow heat and combustion Mechanics,
Gent, Belgium
* Corresponding Author

## ABSTRACT

When modelling low capacity energy systems such as a small (5–150 $kW_{el}$) organic Rankine cycle unit, the governing dynamics are mainly concentrated in the heat exchangers. As a consequence, accuracy and simulation speed of the higher level system model mainly depend on the heat exchanger model formulation. In particular, the modelling of thermodynamic systems characterized by evaporation or condensation, requires heat exchanger models capable of handling phase transitions. To this aim, the finite volume (FV) and the moving boundary (MB) approaches are the most widely used. The two models are developed and included in the open-source ThermoCycle Modelica library. In this contribution a comparison between the two approaches is performed. Their performance is tested in terms of model integrity and accuracy during transient conditions. Furthermore the models are used to simulate the evaporator of an ORC system and their responses are validated against experimental data collected on an 11 $kW_{el}$ ORC power unit.

## 1. INTRODUCTION

The crucial role of dynamic modelling tools in tackling the challenges arising from the unsteady operation of complex physical systems has been generally accepted by the scientific community for the simulation of energy systems (Colonna and van Putten, 2007). Dynamic modelling is considered a reliable tool in energy system design, from evaluating and optimizing the system response time to the development and test of different control strategies. In recent years, the open-access language Modelica (Mattsson and Elmqvist, 1997) has been gaining momentum to be used for dynamic modelling of a wide range of dynamic systems. It allows describing continuous and discrete components in a physical way by writing self-consistent sets of casual and acasual equations, that are then transformed by the tool into an optimized set of hybrid differential-algebraic equations. Various libraries are available to model thermodynamic and thermal-hydraulic systems (Casella and Leva, 2005)with a focus on steam and gas cycles (e.g. ThermoSysPro, PowerPlants, ThermalPower,Thermo Power etc.) or refrigeration systems (e.g. TIL, AirConditioning etc.). Some of these libraries are open-access and only few of them are able to handle non-conventional working fluids thermo-physical properties. The authors recently presented ThermoCycle, a Modelica library targeting the modelling of low-capacity systems (Quoilin et al., 2014b). The library aims at providing a robust and efficient fully open-source suite of models for thermoflow systems, ranging from the computation of thermo-physical substance, through the coupling with the open-source CoolProp software (Bell et al., 2014), to the simulation of complex systems

together with their control strategies. When modelling low capacity systems, the governing dynamic is usually mainly concentrated in the heat exchanger (HE). In the particular case of heat exchangers involving two-phase flows, two commonly adopted HE modelling approaches are the finite volume (FV) and the moving boundary (MB) (Bendapudi et al., 2005). Both methods are based on the conservation laws of physics, where the governing dynamics are expressed in form of the conservation laws of energy, mass and momentum over a defined control volume. In a moving boundary model the fluid flow in the HE is divided in as many control volumes as the states (e.g. liquid, two-phase, vapour) in the fluid flow (in this work: from one to three). The control volumes size varies in time during transients, following the saturated liquid and the saturated vapour boundaries. The finite volume approach consists in discretizing the HE volume in a number of equal and constant control volumes. The conservation laws are then applied in each of the control volumes. The MB and FV methods have been applied starting from the late 70's for thermal system modelling (Dhar and Soedel, 1979) (MacArtur and Grald, 1987). The MB approach result in faster but sometimes less robust models (Bendapudi et al., 2005). Comprehensive literatures reviews by Bendapudi (2002), or Bonilla et al. (2015) show that moving boundary models have been proposed in several studies, but remain less common than FV models. A recent work from Bonilla et al. (2015) reports a clear review of the major MB heat exchanger models capable of handling two-phase flow, and presents a moving boundary library developed in the Modelica language for the modelling of direct steam generation parabolic through solar collectors.
This contribution presents a comparison between the MB and FV approaches to model heat exchanger components in a small capacity organic Rankine cycle (ORC) system. To that aim, the two types of heat exchanger model are developed in the Modelica language and are included into the open-source ThermoCycle library. The models are developed following an object oriented approach while minimizing the Modelica inheritance feature as to enhance model readability. In section 2 the modelling approach, the structure and the main characteristic of these models are presented. A comparison between the two approaches is analysed in section 3 in terms of model integrity by checking the mass and energy balance over a defined simulation time, and of model accuracy by comparing the outlet temperature and mass flow rate, considering as a reference a 100-control volumes (CVs) FV model proposed in Quoilin et al. (2014a). The capability of both models to be integrated in a higher level system model is assessed by using both approaches to simulate the evaporator of an organic Rankine cycle (ORC) unit model. In section 4 the ORC model is validated using transient experimental data from an 11 $kW_{el}$ ORC test-rig equipped with a single screw expander. The results are finally summarized in section 5 and some concluding remarks are formulated.

## 2. HEAT EXCHANGER MODELLING

In this section the finite volume and the moving boundary models developed in the framework of the open-source ThermoCycle Modelica library are presented. The common assumptions considered for both the finite volume and the moving boundary approaches are reported in subsection 2.1. The structure and the governing equations for the MB and the FV models are described in subsection 2.2 and 2.3 respectively.

### 2.1 Assumptions

The heat exchanger models presented in this work are conceived to be integrated into a system model as one of the various components constituting the thermo-hydraulic system. The following assumptions are considered:

- The fluid flow through a control volume of the heat exchanger is described with a mathematical formulation of the conservation laws of physics: dynamic energy and mass balance, static momentum balance.
- The heat exchanger is considered as a 1-dimensional tube (z-direction) through which the working fluid flows.

- Kinetic energy, gravitational forces and viscous stresses are neglected.
- No work is done on or generated by the control volume.
- The velocity of the fluid is uniform over the cross sectional area (homogeneous two-phase flow).
- Pressure drop through the heat exchanger are neglected (constant pressure).
- The rate of thermal energy addition due to heat conduction is neglected in the fluid.
- The rate of thermal energy exchanged with the ambience by convection is considered.
- Thermal energy accumulation is considered for the metal wall of the tube.
- Thermal energy conduction in the metal wall is neglected in the circumferential and axial (z) direction.

### 2.2 Finite volume model

The finite volume heat exchanger model is object oriented, its structure being shown in Figure 1a. It is based on the connection of different subcomponents from the ThermoCycle library. Two fluid components simulating the flow of the fluid in the two sides of the heat exchanger and one wall component representing thermal energy accumulation in the metal wall. The conservation law of physics, describing the behaviour of the fluid through the heat exchanger, are derived by integrating the general 1-dimensional form of mass, energy and momentum balance over a constant volume. Considering the above mentioned assumptions, their final formulation for each CV is reported in Equations 1 to 3.

$$\frac{dM}{dt} = \dot{m}_{\text{su}} - \dot{m}_{\text{ex}} \quad \text{with} \quad \frac{dM}{dt} = V \cdot \left( \frac{\partial \rho}{\partial h} \cdot \frac{dh}{dt} + \frac{\partial \rho}{\partial p} \cdot \frac{dp}{dt} \right) \tag{1}$$

$$V\rho \frac{dh}{dt} = \dot{m}_{\text{su}} \cdot (h_{\text{su}} - h) - \dot{m}_{\text{ex}} \cdot (h_{\text{ex}} - h) + V\frac{dp}{dt} + A_{\text{l}} \cdot \dot{q} \tag{2}$$

$$p_{\text{su}} = p_{\text{ex}} \tag{3}$$

where $\frac{\partial \rho}{\partial h}$ and $\frac{\partial \rho}{\partial p}$ in Equation 1 are considered to be thermodynamic properties of the fluid and are directly computed by the CoolProp library. The "su" (supply) and "ex" (exhaust) subscripts denote the nodes variable of each cell, $A_{\text{l}}$ is the lateral surface through which the heat flux $\dot{q}$ is exchanged with the metal wall and V is the constant volume of each cell. Enthalpy and pressure at the center of the control volume are considered as the state variables. Thermal energy accumulation in the metal wall is expressed as:

$$M_{\text{w}}/N \cdot c_{\text{w}} \cdot \frac{dT_{\text{w}}}{dt} = A_{\text{ext}} \cdot \dot{q}_{\text{ext}} + A_{\text{int}} \cdot \dot{q}_{\text{int}} \tag{4}$$

where $M_{\text{w}}$ is the total mass of the metal wall, N is the number of cells and $c_{\text{w}}$ is the metal wall specific heat capacity. The secondary fluid is modelled as an incompressible fluid whose density and specific heat capacity are assumed constant within the heat exchanger length. The heat transfer through secondary fluid - wall and wall - working fluid is modelled with Newton's law of cooling. Both central and upwind discretization schemes are supported by the model.

### 2.3 Moving boundary model

The moving boundary model is developed following the object-oriented principles of abstraction, encapsulation and (limited) inheritance: two basic models are derived representing the fluid flow through a variable control volume in single and two phase state. The connection of these two basic models allows building dry, flooded or general evaporator and condenser models. The enthalpy of the fluid is assumed linear in each region of the tube (sub-cooled, two-phase, super-heated) and is computed as shown in Equation 5.

$$\overline{h} = \frac{1}{2} \cdot (h_{\text{a}} + h_{\text{b}}) \tag{5}$$

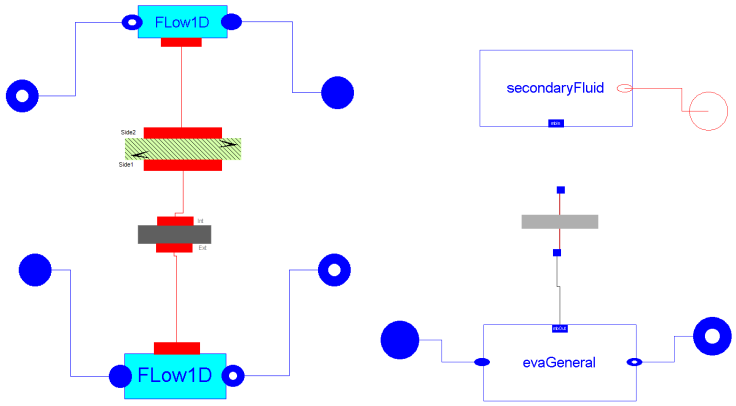


**(a)** **(b)**

**Figure 1: Representation of the finite volume (a) and the moving boundary (b) heat exchanger from the Dymola GUI.**

where a and b subscripts denote the left and right boundaries of the region. Given a moving boundary control volume the mass and energy balance are defined by integrating the general conservation laws of physics over the length of the zone, as shown in Equations 6 and 7

$$A \cdot \int_{l_a}^{l_b} \frac{\partial \rho}{\partial t} \, \mathrm{d}z + \int_{l_a}^{l_b} \frac{\partial \dot{m}}{\partial z} \, \mathrm{d}z = 0 \tag{6}$$

$$A \cdot \int_{l_a}^{l_b} \frac{\partial \left(\rho \cdot h\right)}{\partial t} \, \mathrm{d}z - A \cdot l \cdot \frac{dp}{dt} + \int_{l_a}^{l_b} \frac{\partial \left(h \cdot \dot{m}\right)}{\partial z} \, \mathrm{d}z = dl \cdot Y \cdot \dot{q} \tag{7}$$

where $A$ is the cross sectional area, $l_a$ and $l_b$ are the lengths of the left and right boundaries of the region and $Y$ is the channel perimeter. Assuming a constant pressure, the momentum balance is represented by Equation 3. As far as the one-phase region is concerned, the mass balance is derived solving Equation 6 by applying Leibniz rule to the first term and using the mean-value theorem such that the rate of mass flow change results in:

$$\frac{d}{dt} \int_{l_a}^{l_b} \rho \, \mathrm{d}t = \frac{d}{dt} \left(\overline{\rho} \cdot l\right) \tag{8}$$

the mass balance for a one-phase region is equal to:

$$A \cdot \left[\overline{\rho} \cdot \frac{dl}{dt} + l \cdot \frac{d\overline{\rho}}{dt} - \rho_a \cdot \frac{dl_a}{dt} + \rho_b \cdot \frac{dl_b}{dt}\right] = \dot{m}_a - \dot{m}_b \tag{9}$$

where $\overline{\rho}$ is the average density of the region computed as a function of the pressure and of the average specific enthalpy, $\overline{\rho} \approx f\left(\overline{h}, p\right)$, $l$ is the length of the region and $\frac{d\overline{\rho}}{dt}$ is calculated as:

$$\frac{d\overline{\rho}}{dt} = \frac{\partial \overline{\rho}}{\partial p} \cdot \frac{dp}{dt} + \frac{\partial \overline{\rho}}{\partial \overline{h}} \cdot \frac{d\overline{h}}{dt} = \frac{\partial \overline{\rho}}{\partial p} \cdot \frac{dp}{dt} + \frac{1}{2} \cdot \frac{\partial \overline{\rho}}{\partial \overline{h}} \cdot \left(\frac{dh_a}{dt} + \frac{dh_b}{dt}\right) \tag{10}$$

where $\frac{dh_{b/a}}{dt}$ are defined based on Equations 11 to 14 reported in Table 1. The energy balance is derived from equation Equation 7. Applying Leibniz rule to the first term and using the mean-value theorem allows to define the rate of energy change as:

$$\frac{d}{dt} \int_{l_a}^{l_b} \left(\rho \cdot h\right) \, \mathrm{d}z = \frac{d}{dt} \left(\overline{\rho h} \cdot l\right) \approx \frac{d}{dt} \left(\overline{\rho} \cdot \overline{h} \cdot l\right) \tag{15}$$

with $\overline{\rho h} \approx \overline{\rho} \cdot \overline{h}$. The energy balance for the one-phase region results in:

$$A \cdot \left[\overline{\rho}\overline{h}\frac{dl}{dt} + \overline{h}l\frac{d\overline{\rho}}{dt} + \overline{\rho}l\frac{d\overline{h}}{dt} + \left(\rho_a h_a\right) \cdot \frac{dl_a}{dt} - \left(\rho_b h_b\right) \cdot \frac{dl_b}{dt}\right] - A \cdot l_a \cdot \frac{dp}{dt} = \dot{m}_a \cdot h_a - \dot{m}_b \cdot h_b + \dot{Q} \tag{16}$$

**Table 1: Specific boundary enthalpy derivative depending on the heat transfer and control volume.**

| | Evaporator | | Condenser | |
|---|---|---|---|---|
| Sub-cooled | $\frac{dh_\mathrm{b}}{dt} = \frac{\partial h_\mathrm{l}}{\partial p}\frac{dp}{dt}$ | (11) | $\frac{dh_\mathrm{a}}{dt} = \frac{\partial h_\mathrm{l}}{\partial p}\frac{dp}{dt}$ | (12) |
| Super-heated | $\frac{dh_\mathrm{a}}{dt} = \frac{\partial h_\mathrm{v}}{\partial p}\frac{dp}{dt}$ | (13) | $\frac{dh_\mathrm{b}}{dt} = \frac{\partial h_\mathrm{v}}{\partial p}\frac{dp}{dt}$ | (14) |

In the two-phase region, the assumption of homogeneous two-phase flow condition allows to express the mean density as a function of the average void fraction $\overline{\gamma}$ as:

$$\overline{\rho} = (1-\overline{\gamma})\,\rho_\mathrm{l} + \overline{\gamma}\rho_\mathrm{v} \tag{17}$$

where the average void fraction is calculated integrating the local void fraction $\gamma$ over the length of the region. $\overline{\gamma}$ is an indicator of the fraction of the total volume of the region occupied by fluid in vapour phase (Jensen, 2003). Substituting Equation 17 into Equation 8 and solving Equation 6 results in the mass balance for the two phase region:

$$A\left[((1-\overline{\gamma})\rho_\mathrm{l} + \overline{\gamma}\rho_\mathrm{v})\frac{dl}{dt} + l\left((\rho_\mathrm{v}-\rho_\mathrm{l})\frac{d\overline{\gamma}}{dt} + \overline{\gamma}\frac{d\rho_\mathrm{v}}{dp}\frac{dp}{dt} + (1-\overline{\gamma})\frac{d\rho_\mathrm{l}}{dt}\right) - \rho_\mathrm{a}\frac{dl_\mathrm{a}}{dt} + \rho_\mathrm{b}\frac{dl_\mathrm{b}}{dt}\right] = \dot{m}_\mathrm{a} - \dot{m}_\mathrm{b} \tag{18}$$

The energy balance for the two phase region is obtained from Equation 7 using Equations 17 and 15:

$$\begin{aligned} A\Bigg[((1-\overline{\gamma})\,\rho_\mathrm{l}h_\mathrm{l} + \overline{\gamma}\rho_\mathrm{v}h_\mathrm{v})\frac{dl}{dt} + l\left((\rho_\mathrm{v}h_\mathrm{v}-\rho_\mathrm{l}h_\mathrm{l})\frac{d\overline{\gamma}}{dt} + \overline{\gamma}h_\mathrm{v}\frac{\partial\rho_\mathrm{v}}{\partial p}\frac{dp}{dt} + \overline{\gamma}\rho_\mathrm{v}\frac{\partial h_\mathrm{v}}{dp}\frac{dp}{dt}\right. \\ \left. + (1-\overline{\gamma})\,h_\mathrm{l}\frac{\partial\rho_\mathrm{l}}{dp}\frac{dp}{dt} + (1-\gamma)\,\rho_\mathrm{l}\frac{\partial h_\mathrm{l}}{\partial p}\frac{dp}{dt}\right) + (\rho_\mathrm{a}h_\mathrm{a})\frac{dl_\mathrm{a}}{dt} - (\rho_\mathrm{b}h_\mathrm{b})\frac{dl_\mathrm{b}}{dt}\Bigg] - A\cdot l\cdot\frac{dp}{dt} \\ = \dot{m}_\mathrm{a}h_\mathrm{a} - \dot{m}_\mathrm{b}h_\mathrm{b} + \dot{Q} \end{aligned} \tag{19}$$

The option of imposing a constant average void fraction, i.e. $\frac{d\overline{\gamma}}{dt} = 0$ , is supported by the model. The MB with constant void fraction is abbreviated as MBConstVF. The effect of such an assumption is analysed in section 4. The thermal energy balance in the metal wall for each control volume is expressed as:

$$\rho_\mathrm{w}c_\mathrm{w}A_\mathbf{w}\frac{\partial T_\mathrm{w}}{\partial t} = dl\cdot Y\cdot\dot{q}_\mathrm{wf} + dl\cdot Y\cdot\dot{q}_\mathrm{sf} \tag{20}$$

Applying Leibniz rule and solving the integral results in:

$$\rho_\mathrm{w}c_\mathrm{w}A_\mathrm{w}\left[\frac{d}{dt}\int_{l_\mathrm{a}}^{l_\mathrm{b}}\partial T_\mathrm{w}\,\mathrm{d}z + T_\mathrm{w}\,(l_\mathrm{b})\frac{dl_\mathrm{b}}{dt} - T_\mathrm{w}\left(l_\mathrm{a}\frac{dl_\mathrm{a}}{dt}\right)\right] = \dot{Q}_\mathrm{wf} + \dot{Q}_\mathrm{sf} \tag{21}$$

In order to simplify the resolution of the model, no energy, mass and momentum accumulation is considered in the secondary fluid. A linear temperature distribution is assumed and the thermal energy transfer with the metal wall is solved either with the semi-isothermal $\varepsilon$-NTU method or with Newton's law of cooling.

## 3. MODEL INTEGRITY

In this section a comparison between the FV and MB approach is performed with the aim of testing the model accuracy and integrity. The accuracy is defined as the agreement of the model-predicted output values with a reference system. The integrity is defined as the capacity of the model of respecting the

conservation of energy and mass. The FV and MB evaporator models are subjected to inlet enthalpy and pressure variations, whose value is limited to avoid any back-flow or any phase change at the working fluid outlet. The boundary conditions for pressure and enthalpy are defined in Equations 22 and 23.

$$p = 8.04 + 0.2 \cdot \sin\left(0.1 \cdot 2\pi \cdot t\right) \text{[bar]} \tag{22}$$

$$h_{\text{su}} = 0.11 \cdot 10^5 + 0.2 \cdot 10^5 \cdot sin\left(0.2 \cdot 2\pi \cdot t\right) \text{[J/kg]} \tag{23}$$

The FV heat exchanger model is discretized using the upwind method and simulations are performed considering 10, 20, 40 and 100 CVs. The medium selected for these simulations is Solkatherm (SES36). The simulation is initialized in steady-state and lasts 625 seconds. The numerical solver is the DASSL and the relative tolerance is set to $10^{-4}$. The integrity of the models is investigated by calculating the energy and mass balances over the whole simulation time for each model unit. The energy balance over each heat exchanger model is computed as:

$$\varepsilon_{\text{ener}} = \frac{\left(E_{\text{ext}} + E_{\text{su}} - E_{\text{ex}} - \Delta U\right)_{\text{wf}} + \left(E_{\text{ext}} + E_{\text{su}} - E_{\text{ex}} - \Delta U\right)_{\text{sf}} + \left(E_{\text{inlet}} - E_{\text{outlet}} - \Delta U\right)_{\text{wall}}}{E_{\text{ext,sf}}} \tag{24}$$

where $E_{\text{ext}}$ is the overall thermal energy exchanged due to heat convection through the lateral surface, $E_{\text{ex/su}}$ is the total energy into/out of the system due to leaving/entering mass flow rate and $\Delta U$ is the total net increase of energy. They are calculated in Equation 25.

$$E_{\text{ext}} = \int_0^t \dot{Q}\,\mathrm{d}t\,, \quad E_{\text{ex/su}} = \int_0^t \dot{m}_{\text{ex/su}} \cdot h_{\text{ex/su}}\,\mathrm{d}t\,, \quad \Delta U = \int_0^t \left(U_{\text{final}} - U_{\text{init}}\right)\,\mathrm{d}t \tag{25}$$

The conservation of mass is checked on the working fluid side as:

$$\varepsilon_{\text{mass}} = \sum_{i=1}^{n} \frac{M_{\text{ex}} - M_{\text{su}} - \Delta M}{M_{\text{su}}} \tag{26}$$

where $M_{\text{ex/su}}$ is the overall mass leaving/entering the system and $\Delta M$ is the net change in mass. Their values are computed using Equation 27.

$$M_{\text{ex/su}} = \int_0^t \dot{m}_{\text{ex,su}}\,\mathrm{d}t \quad \Delta M = \int_0^t \left(V\rho_{\text{final}} - V\rho_{\text{init}}\right)\,\mathrm{d}t \tag{27}$$

The accuracy of the models is investigated by comparing the model output enthalpy and mass flow rate with respect to a reference system, using as mathematical indicator the mean percentage relative error, $\overline{\epsilon}$, defined in Equation 28. In this case the finite volume model with 100 CVs is taken as a reference.

$$\epsilon\left(j\right) = 100 \cdot \frac{\left|X_{\text{s}}\left(j\right) - X_{\text{ref}}\left(j\right)\right|}{X_{\text{ref}}\left(j\right)} \quad \epsilon = \sum_{j=1}^{n} \left|\epsilon\left(j\right)\right| \quad \overline{\epsilon} = \frac{\epsilon}{n} \quad j \in [1, n]. \tag{28}$$

where $X_{\text{s}}\left(j\right)$ and $X_{\text{ref}}\left(j\right)$ are the j*th* sampled simulation and reference value of the selected variable and n is the number of sampling. Table 2 reports the benchmarking indicators for the integrity and accuracy simulations for the MB and FV models. The error on conservation of mass and energy balance is kept low by all the considered models. As expected the computational time increases exponentially with the increase of the number of CVs in the FV model. The MB approach results three order of magnitude faster than the finite volume with 100 CVs, allowing to maintain a good accuracy with respect to the 100 CVs FV model in terms of outlet mass flow and outlet enthalpy as the mean PRE value show. In Figure 2, the temperature profile for heat transfer calculation for the MB and FV model is depicted.

## 4. VALIDATION

In this section, the integration of the FV and MB heat exchanger models into a larger system model is validated against transient experimental data recorded on a 11 $\text{kW}_{\text{el}}$ ORC unit. In subsection 4.1, the ORC test rig used to collect the experimental data is presented. subsection 4.2, reports a brief description of the different dynamic model components used to represent the whole ORC system. In subsection 4.3 the validation results are analysed.

**Table 2: Benchmarking indicators for the integrity and accuracy test for the moving boundary and the finite volume models.**

| Model | MBConstVF | MB | FV 10 CVs | FV 20 CVs | FV 40 CVs | FV 100 CVs |
|---|---|---|---|---|---|---|
| $\varepsilon_{\text{mass}}$ [%] | $2.33 \cdot 10^{-13}$ | $1.08 \cdot 10^{-12}$ | $1.72 \cdot 10^{-13}$ | $6.33 \cdot 10^{-13}$ | $3.06 \cdot 10^{-14}$ | $1.01 \cdot 10^{-12}$ |
| $\varepsilon_{\text{ener}}$ [%] | $6.67 \cdot 10^{-12}$ | $9.51 \cdot 10^{-12}$ | $5.28 \cdot 10^{-12}$ | $2.89 \cdot 10^{-12}$ | $4.64 \cdot 10^{-12}$ | $1.04 \cdot 10^{-12}$ |
| $\bar{\epsilon}\ h_{\text{ex}}$ [%] | 0.55 | 0.69 | 3.16 | 1.06 | 0.31 | 0.0 |
| $\bar{\epsilon}\ \dot{m}_{\text{ex}}$ [%] | 3.88 | 1.40 | 5.52 | 1.85 | 0.53 | 0.0 |
| Time [s] | 0.65 | 0.73 | 2.89 | 13.7 | 34.8 | 147 |

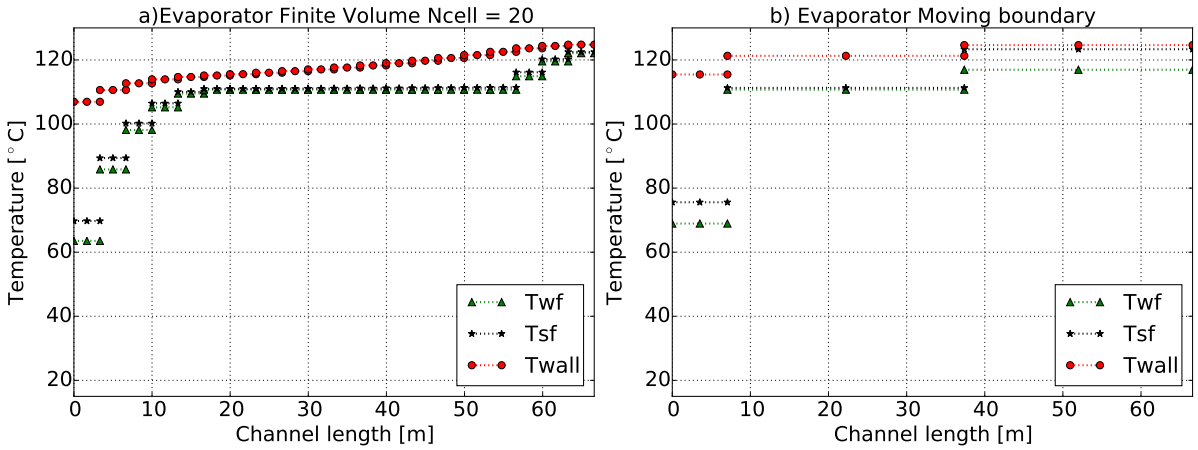


**Figure 2: Temperature profile for heat transfer calculation in the finite volume and the moving boundary model. Each segment corresponds to one control volume.**

### 4.1 ORC test rig facility

The ORC set-up used to acquire the experimental data for dynamic model validation is depicted in Figure 3a. The system is equipped with a single screw expander with a nominal shaft power of 11 kW. The same brazed plate heat exchanger type is used for the evaporator, recuperator and condenser. SES36 is the selected working fluid. Sensors are placed at the inlet and at the outlet of each ORC unit component. For further information on the test-rig, the range and the precision of the measurement devices the interested reader can refer to (Desideri et al., 2015).

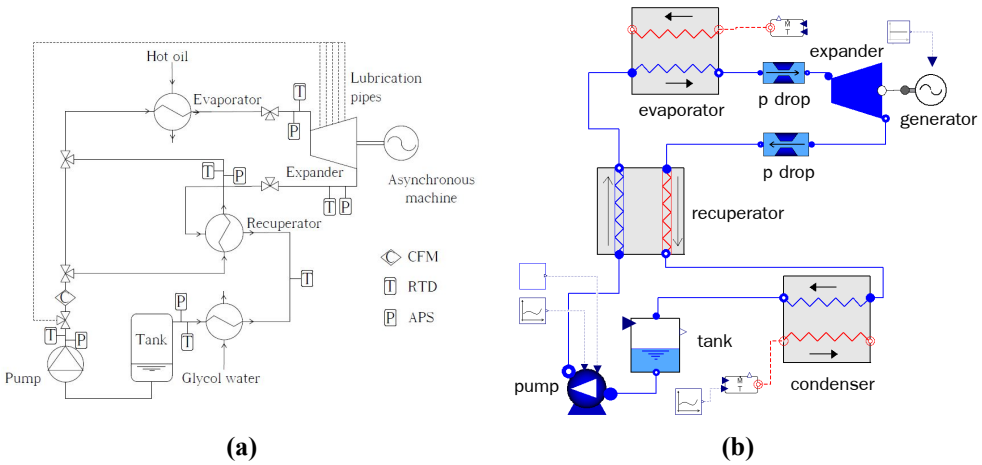


**Figure 3: Process flow diagram of the ORC with sensors position (a). ORC system model from the Modelica-Dymola GUI.**

### 4.2 ORC system modelica model

When modelling a low-capacity power unit, since the time constants characterizing the expansion and compression processes are small compared to those of the heat exchangers, semi-empirical (or lumped parameter) steady-state models can be used to simulate the expander and the pump components. The expansion machine is modelled by its effectiveness, expressed with a formulation proposed by Declaye et al. (2013), and the filling factor. The pump model is based on two empirical correlations, one for the effectiveness as a function of the pressure ratio and the pump speed, and one for the delivered mass flow rate as a function of the pump speed. The empirical coefficients for the different performance curves have been derived based on the acquired measurements of the test unit. A more detailed description of this process together with the values of the coefficients is reported in Desideri et al. (2014). The tank at the condenser outlet is modelled assuming thermodynamic equilibrium at all times and accounting for mass and energy accumulation. A lumped approach is applied for pressure drop modelling. Two pressure drop components are placed at the lowest vapour density part of both the low and high pressure lines accounting for laminar and turbulent phenomena. Finally the recuperator and the condenser components are modelled with the finite volume model. The evaporator is modelled using both the finite volume and the moving boundary to investigate the difference between the two approaches at a system level. The ORC model layout is shown in Figure 3b from the Modelica-Dymola graphical user interface.

### 4.3 Model validation

The transient response of the ORC unit is investigated by applying a downward step of 5 Hz to the pump rotational speed starting from a steady-state condition. The effectiveness of the finite volume and the moving boundary model is checked by replicating the pump step change experiment on the developed Modelica ORC model, using as an evaporator the finite volume and the moving boundary model. The

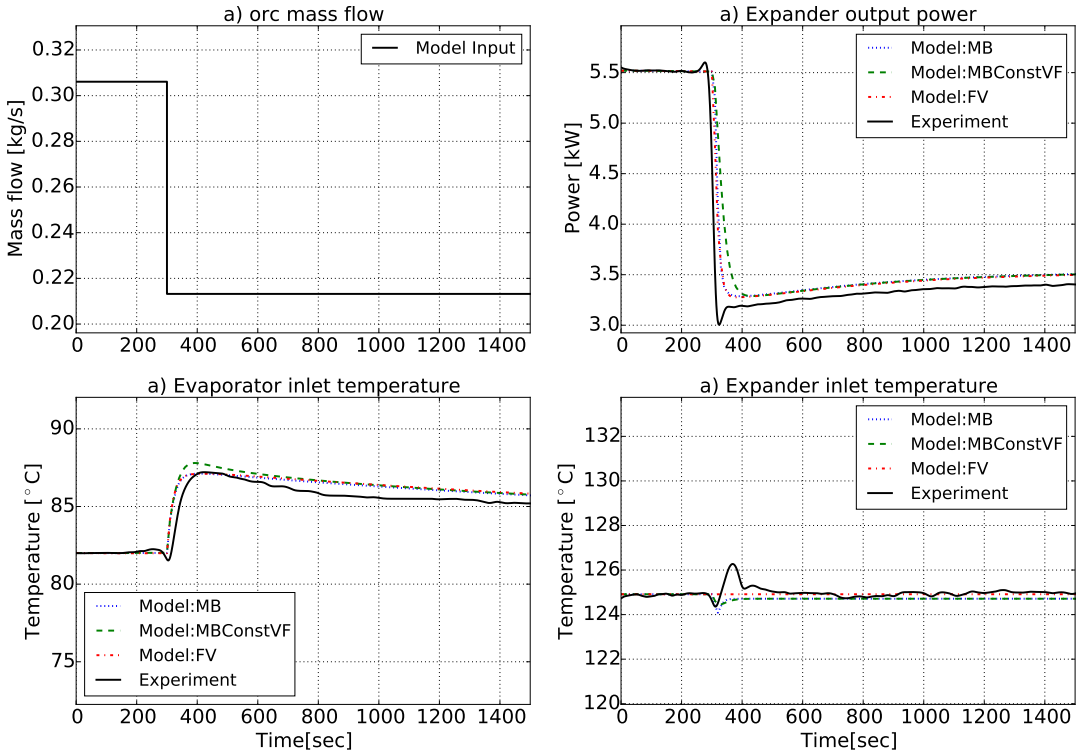


**Figure 4: Downward-Upward 5 Hz step change to the pump rotational speed.**

results are shown in Figure 4. The step down happens at t=300 seconds. Both models are able to well replicate the dynamics characterizing the system. It is interesting to note that when the void fraction is kept constant in the MB model, MBConstFV, the response of the model is slower compared to that of the real unit. This is explained by the fact that when the mass flow decreases the void fraction increases as

the portion of area occupied by the gas increases. As a consequence the thermal capacity decreases and this results in faster transients. Keeping the void fraction constant neglect such a phenomena resulting in a too slow response. It also results in a poor prediction of the outlet flow rate variations during transients.

## 5. CONCLUSIONS

In this work a comparison between the finite volume and moving boundary approach to model an evaporator is proposed. An integrity and stability test for each approach has been performed taking as benchmarking indicator the simulation speed, the conservation of mass and energy and the mean percentage relative error, $\overline{\epsilon}$, for outlet enthalpy and mass flow rate with respect to a 100 CVs finite volume. The FV and MB models are used in the Modelica model of an ORC system to simulate the evaporator component. The transient response of the model is compared against experimental results. The main outcomes of this study are summarized hereunder:

- The integrity test results allow to conclude that both the MB and FV approaches are well suited for modelling dynamic heat exchanger being characterized by a low error on the total conservation of energy and mass. Further, the MB is 3 orders of magnitude faster compared to a finite volume with a 100 CVs.
- The comparison against experimental transients demonstrates that the assumptions of constant void fraction in the MB approach overestimate the dynamics (i.e. leads to slower response times) making it unsuitable for modelling small capacity heat exchanger.

The proposed MB and FV models together with the test cases are open source and are available in the latest version of the ThermoCycle library. An experimental campaign focusing on the investigation of the specific dynamics characterizing the evaporator and condenser components is planned. The recorded data will be used to perform a more detailed validation of the FV and MB approach for modelling small capacity heat exchangers.

## NOMENCLATURE

| | | | | | |
|---|---|---|---|---|---|
| FV | Finite volume | | $T$ | Temperature | (°C) |
| MB | Moving boundary | | $t$ | Time | (sec) |
| CV | Control volume | | $l$ | Control volume length | (m) |
| n | samples time | | $\rho$ | Density | ($kg.m^{-3}$) |
| | | | $\dot{m}$ | Mass flow rate | ($kg.s^{-1}$) |
| **Subscript** | | | $h$ | Specific enthalpy | ($kJ.kg^{-1}$) |
| ex | Exit | | $E$ | Energy | (kJ) |
| su | Supply | | $U$ | Internal energy | (kJ) |
| ext | External | | $\dot{Q}$ | Thermal power | (kW) |
| v | Saturated vapor state | | $\dot{q}$ | heat flux | ($kW.m^{-1}$) |
| l | Saturated liquid state | | $Y$ | Channel perimeter | (m) |
| | | | $\dot{m}$ | Mass flow | ($kg.s^{-1}$) |
| **Symbols** | | | $\gamma$ | Void fraction | |
| $p$ | Pressure | (bar) | $\epsilon$ | Relative error | |

## REFERENCES

I.H. Bell, J. Wronski, S. Quoilin, and V. Lemort. Pure- and pseudo-pure fluid thermophysical property evaluation and the open-source thermophysical property library CoolProp. *Industrial & Engineering Chemistry Research*, 53:2498–2508, 2014.

S. Bendapudi. A literature review of dynamic models of vapor compression equipment. Technical report, Herrick Laboratories, Purdue University, 2002.

S. Bendapudi, J. Braun, E. Groll, and A. Eckhard. Dynamic model of a centrifugal chiller system–model development, numerical study and validation. *ASHRAE*, 2005.

Javier Bonilla, Sebastian Dormido, and Francois E. Cellier. Switching moving boundary models for two-phase flow evaporators and condensers. *Communications in Nonlinear Science and Numerical Simulation*, 20(3):743–768, 2015. ISSN 1007-5704.

F. Casella and A. Leva. Object-oriented modelling & simulation of power plants with modelica. In *Proceedings of the 44th IEEE Conference on Decision and Control, and the European Control Conference*, 2005.

P. Colonna and H. van Putten. Dynamic modeling of steam power cycles.: Part I—modeling paradigm and validation. *Applied Thermal Engineering*, 27(2–3):467–480, 2007. ISSN 1359-4311.

Sebastien Declaye, Sylvain Quoilin, Ludovic Guillaume, and Vincent Lemort. Experimental study on an open-drive scroll expander integrated into an ORC (organic Rankine cycle) system with R245fa as working fluid. *Energy*, 55(0):173–183, 2013. ISSN 0360-5442.

A. Desideri, M. v. d. Broek, S. Gusev, V. Lemort, and S. Quoilin. Experimental campaign and modeling of a low-capacity waste heat recovery system based on a single screw expander. In *22nd International compressor engineering conference at Purdue*, 2014.

A. Desideri, S. Gusev, M. v.d. Broek, V. Lemort, and S. Quoilin. Experimental comparison of organic fluids for low temperature ORC systems for waste heat recovery applications. *Energy Submitted for publications*, xx:xx, 2015.

M. Dhar and W. Soedel. Transient analysis of a vapor compression refrigeration system. In *In proceedings of the XV International Congress of Refrigeration*, Venice, 1979.

Jakob Munch Jensen. *Dynamic Modeling of Thermo-Fluid Systems*. PhD thesis, Technical University of Denmark, 2003.

J.W. MacArtur and E.W. Grald. Prediction of cyclic heat pump performance with a fully distributed model and a comparison with experimental data. *ASHRAE Transactions*, 93(2):1159–1178, 1987.

S.E. Mattsson and H. Elmqvist. Modelica - an international effort to design the next generation modeling language. In *Proceedings of the 7th IFAC Symposium on Computer Aided Control Systems Design*, 1997.

S. Quoilin, I. H. Bell, A. Desideri, P. Dewallef, and V. Lemort. Methods to Increase the Robustness of Finite-Volume Flow Models in Thermodynamic Systems. *Energies*, 7:1621–1640, 2014a.

S. Quoilin, A. Desideri, J. Wronski, I. H. Bell, and V. Lemort. ThermoCycle: A Modelica library for the simulation of thermodynamic systems. In *Proceedings of the 10th International Modelica Conference*, 2014b.

## ACKNOWLEDGEMENT

The results presented in this paper have been obtained within the frame of the IWT SBO-110006 project The Next Generation Organic Rankine Cycles (www.orcnext.be), funded by the Institute for the Promotion and Innovation by Science and Technology in Flanders. This financial support is gratefully acknowledged.